Combining inter-source seismic interferometry and source-receiver interferometry for deep local imaging

Yi Liu, Norwegian University of Science and Technology; Kees Wapenaar and Joost van der Neut, Delft University of Technology; Børge Arntsen, Norwegian University of Science and Technology*

Summary

The virtual source method has been applied successfully to retrieve the impulse response between pairs of receivers in the subsurface. This method is further improved by an up-down separation prior to the crosscorrelation to suppress the reflections from the overburden and the free surface.
In a reversed situation where the sources are in the subsurface and receivers are on the surface, in principle, one can apply the same logic to retrieve the virtual response between pairs of sources by source-receiver reciprocity, turning the physical borehole sources into virtual receivers. However, since the up-down separation is not applicable on the source side, the simple crosscorrelation of the total fields results in spurious events due to the incomplete receiver coverage around the sources. We show with a numerical example that for this configuration of borehole sources and surface receivers, one can replace such an up-down separation at the source side by that of the direct and reflected waves as a first order approximation. This procedure produces the virtual receiver data that is adequate for local imaging below the source depth and is completely independent of the accuracy of the overburden velocity model. We implement this inter-source type of interferometry by multidimensional deconvolution (MDD). Further, if the conventional surface survey data is available, we test the methodology from source-receiver interferometry (SRI) for this reverse configuration with borehole sources to retrieve the virtual receiver data with reflections coming from above, using also only the separation of the direct and reflected waves. By migrating the two sets of virtual receiver data, one can create a local image around the borehole sources in a deep area with better focusing and localization without a sophisticated velocity model.

Introduction

Most seismic exploration images are made using surface seismic data. In deeper areas with a complex overburden, borehole seismic data can provide the extra structural information that is hard to extract from surface data. Seismic interferometry (SI) (Schuster et al., 2004; Wapenaar and Fokkema, 2006; Curtis et al., 2006) opens possibilities for transforming borehole seismic data into various forms of acquisition geometries, providing extra illumination of the subsurface structures.

The virtual source method is first illustrated by Bakulin and Calvert (2004, 2006), who use crosscorrelation to turn receivers in a horizontal borehole below a complex overburden into virtual sources, removing interferences from the overburden. The process does not require any knowledge of the material parameters of the overburden. If the dual-field measurements is available in the borehole, a p-z (pressure and vertical velocity component) combination can be used to separate the upgoing from downgoing waves before crosscorrelation, an approach illustrated by Metha et al. (2007) to improve the virtual source data. Vasconcelos et al. (2008) introduce target-oriented interferometry by selecting the directions of waves between receivers using shot-domain wavenumber separation. All above implementations can be referred as inter-receiver SI, as the virtual response is retrieved between receivers. Spurious events are introduced because in practice the source aperture is limited and there is only one-sided illumination from the sources (Snieder et al., 2006).

In a reversed situation where the virtual response is retrieved between sources, this type of interferometry is referred as inter-source SI (Curtis et al., 2009). This type of interferometry can be used to transform a reverse VSP into a survey with both sources and receivers in the subsurface. However, as the correlation gather is summed over the receivers on the surface in this case and one usually has more receivers than sources, the stationary points can be more easily captured. Liu et al. (2013) show a numerical example of this type of interferometry, implemented as interferometry by multidimensional deconvolution (MDD).

Curtis and Halliday (2010) propose SRI to construct the wavefield between a source and a receiver using recordings to or from the two surrounding boundaries. It allows one to incorporate the more conventional seismic data for use in interferometry. Poliannikov (2011) uses SRI to recover the reflection from above the borehole receivers.

By extending the idea behind the virtual source method (Bakulin and Calvert, 2006) to a reverse configuration with borehole sources, we use a representation of inter-source SI by MDD (Liu et al., 2013; van der Neut et al., 2011; Wapenaar et al., 2011) to create the virtual receiver data with reflection from below. Further, by adding the more commonly available surface seismic data for use in SRI, we show that one can also retrieve the virtual receiver data with reflections from above. This process, as previously mentioned, does not require any model parameters of the medium, and is completely data driven. It only requires the separation of the direct arrivals from the reflections in the data. Compared with a conventional surface seismic image, the virtual receiver data can produce a local image of the deeper part of the model without any velocity information of the overburden.

Theory

We start with an acquisition geometry shown in figure 1a. The sources in the borehole are denoted as **x** and the receivers on the surface as **r**. Liu et al. (2013) derived the representation for inter-source SI by MDD for such a geometry in the frequency domain as

$$G^{in}(\mathbf{r}\mid\mathbf{x}_s) = \int G^{out}(\mathbf{r}\mid\mathbf{x})\overline{G}_d^{in}(\mathbf{x}\mid\mathbf{x}_s)d\mathbf{x} \qquad (1)$$

where the superscript *in* and *out* denotes the direction of the waves to or from the sources, as illustrated in Figure 1a. $\overline{G}_d^{in}$ is the dipole Green's function from $\mathbf{x}_s$ to **x** and the bar above means that the medium above the sources is homogeneous. Interferometry by MDD aims at resolving $\overline{G}_d^{in}$ from equation (1).

As a complete separation of the incoming and outgoing waves at the source level **x** is not available, we approximate the outgoing component with the direct waves, and the incoming component with the remaining data, a similar approach as in Bakulin and Calvert (2006). Then by adopting the same matrix convention (Berkhout, 1982) used in Wapenaar et al. (2008), where each column represents one source and each row represents one receiver, one can replace the integral by matrix multiplication:

$$\mathbf{G}^{in} = \mathbf{G}^{out}\overline{\mathbf{G}}_{MDD} \qquad (2)$$

Here we rewrite the unknown dipole Green's function as $\overline{\mathbf{G}}_{MDD}$ to distinguish from the known quantities. To solve it with a least square's approach, we write the normal equation as

$$\mathbf{G}^{out\dagger}\mathbf{G}^{in} = \mathbf{G}^{out\dagger}\mathbf{G}^{out}\overline{\mathbf{G}}_{MDD} \qquad (3)$$

where $\dagger$ denotes the complex conjugate transpose. This also allows us to see the connection between MDD and CC, which says that the CC result (the left-hand side) is equal to $\overline{\mathbf{G}}_{MDD}$ blurred by the point spread function (PSF) represented by $\mathbf{G}^{out\dagger}\mathbf{G}^{out}$ in this formulation. By making the direct arrival approximation explained above, one can see that the left side of the equation is exactly the source-receiver reciprocity counterpart of the virtual source method (Bakulin and Calvert, 2006) and it also resembles the representation for the perturbation wavefield interferometry by Vasconcelos (2008). The unknown can be solved by matrix inversion with a stabilization parameter ε^2, and it contains the correct amplitude and phase of the reflections from below the sources:

$$\overline{\mathbf{G}}_{MDD} = [\mathbf{G}^{out\dagger}\mathbf{G}^{out} + \varepsilon^2\mathbf{I}]^{-1}\mathbf{G}^{out\dagger}\mathbf{G}^{in} \qquad (4)$$

Next, we consider the acquisition geometry in Figure 1b, where a surface survey is included. The source and receiver in the surface survery data are denoted as **s** and **r**. Using a similar approach as Poliannikov (2010) under the framework of SRI (Curtis and Halliday, 2010), an equation for retrieving the reflections from above the sources can be written as

$$\overline{G}^{out}(\mathbf{x}\mid\mathbf{x}_S) = -\int\int G^{out}(\mathbf{r}\mid\mathbf{x})G^{out}(\mathbf{s}\mid\mathbf{x}_S)G^{rs*}(\mathbf{r}\mid\mathbf{s})d\mathbf{r}d\mathbf{s} \quad (5)$$

where *out* is still used with respect to the borehole source surface $\partial\mathbf{x}$; G^{rs} denotes the reflections from above the borehole source depth, with the direct arrivals between **r** and **s** removed; and * denotes complex conjugate. In practice, G^{out} is approximated with the direct arrivals from borehole sources to the surface receivers, and G^{rs} is approximated by selecting the arrivals within the estimated two-way travel time from the borehole source depth to the surface. As the borehole depth and the average P-wave velocity of the medium are available, such an estimation can be made. Again, using the matrix notation, the double integral in equation (5) can be computed efficiently by matrix multiplication as

$$\overline{\mathbf{G}}_{SRI}^{out} = -\mathbf{G}^{out^T}(\mathbf{G}^{rs*}\mathbf{G}^{out}) \qquad (6)$$

Here the superscript ^{T} denotes transpose. This scheme can be understood intuitively from Figure 1b, where the travel time along the red path is subtracted from that along the blue paths.

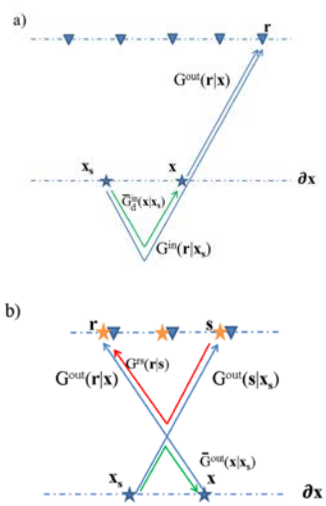

Figure 1: Illustration of the survey geometries. a) The acquisition geometry for the inter-source SI by MDD scheme. b) The acquisition geometry for the SRI scheme. The stars denote sources and the triangles denote receivers. The color green indicates the propagation path for the retrieved virtual response.

Numerical example

We test the method with a numerical example. The model size is 5 by 5 km with a grid sampling of 5 meters. In the borehole case, there are 41 shots evenly placed in a horizontal borehole at a depth of 3.8 km, with a spatial interval of 25 meters. The first shot is at x=2000 m and the last at x=3000 m. The modelled pressure responses are recorded by 101 evenly placed receivers at the surface, with a spatial interval of 50 meters. The first receiver is at x=0 m and the last is at x=5000 m. To model the data for the SRI scheme, 101 shots at the same spatial locations as the surface receivers are used. The data are modelled using a finite difference code presented by Thorbecke and Draganov (2011). The source signal is a Ricker wavelet with 15 Hz peak frequency. The P-wave velocity model is shown in Figure 2, where the locations of the sources and receivers in both cases are indicated.

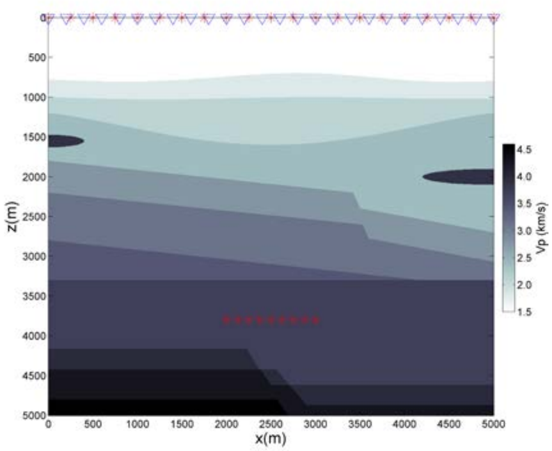

Figure 2: Geometry of the numerical experiment with the velocity model used. The blue triangles denote receivers and the red stars denote sources.

Figure 3 shows the comparison between the reference response and the retrieved virtual response by MDD and SRI, respectively. In Figure 3a, the reference response is modelled with a source at x=2500 m, z=3800 m and recorded by receivers located from x=2000 m to x=3000 m at the depth of 3800 m, essentially turning all sources in the borehole into receivers. However, the overburden in the reference state is homogeneous, with the same velocity as the layer where the borehole sources are located. In Figure 3b, the reference response is modelled with the same geometry as the MDD case, but with the underburden being homogeneous. The overall match is quite good, with the phase information of the reflectors near the borehole sources all captured.

It is suspected that the major descrepancies, seen between 0 s and 0.25 s in Figure 3a and between 1.5 s to 2.5 s in Figure 3b, occur as the consequence of approximating the outgoing waves with the direct waves, instead of all the outgoing waves from the borehole. As the interference from two elliptical shaped high velocity anomalies in the overburden is much stronger than the other outgoing internal multiples, neglecting them contributed to these artifacts in the virtual response.

Figure 4 shows the migrated image using the virtual data, together with the velocity model representing the state in which the virtual data is retrieved as the background. A one-way prestack depth migration is used (Thorbecke et al., 2004). We see in Figure 4a, that indeed one does not need any information of the overburden to image the fault below the sources in the borehole. Figure 4c combines both images in Figure 4a and 4b together, and shows that all reflectors near the borehole sources are well positioned using the two sets of retrieved virtual receiver data. For a general comparison, the surface seismic image is shown in Figure 4d. Note that in order to position the deep reflectors correctly, the surface image is migrated using the whole true velocity model and a denser source and receiver sampling of the surface than the data used in the interferometry experiments.

Conclusions

Inter-source seismic interferometry by multi-dimensional deconvolution allows one to retrieve the impulse response between pairs of sources in the subsurface as if the medium outside of the source surface is homogeneous. The interferometry process does not require any information of the model parameters of the overburden. One advantage of this geometry is that it is easier to have a sufficient receiver coverage on the surface such that the stationary phase positions are covered in order to illuminate the target below. It also might be possible to use the method with active drilling sources for imaging locally while drilling . By applying both classic interferometry of inter-source type and source-receiver interferometry, we present a workflow for turning borehole sources into virtual receivers and imaging around the deep borehole sources. The result shows a well-positioned image in the deep subsurface without a complete velocity model of the overburden.

Acknowledgement

This work is supported by the Deep Imaging and Geo-steering project of the Drilling and Well Centre for Improved Recovery (DrillWell) and the ROSE consortium at Norwegian University of Science and Technology.

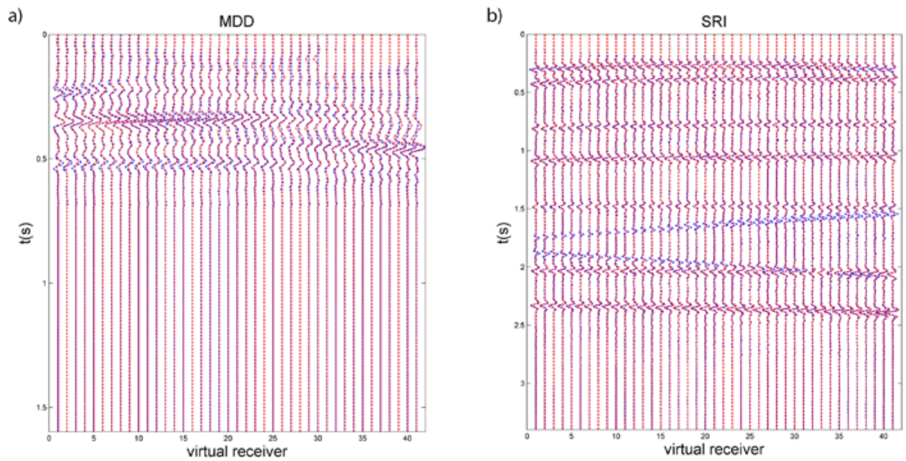

Figure 3: Comparison between the virtual response and the reference response. a) Retrieved response (in red) by inter-source SI using MDD compared with the reference response (in blue) modelled with a homogeneous overburden. b) Retrieved response (in red) by SRI compared with the reference response (in blue) modelled with a homogeneous underburden. The direct waves are removed in both panels.

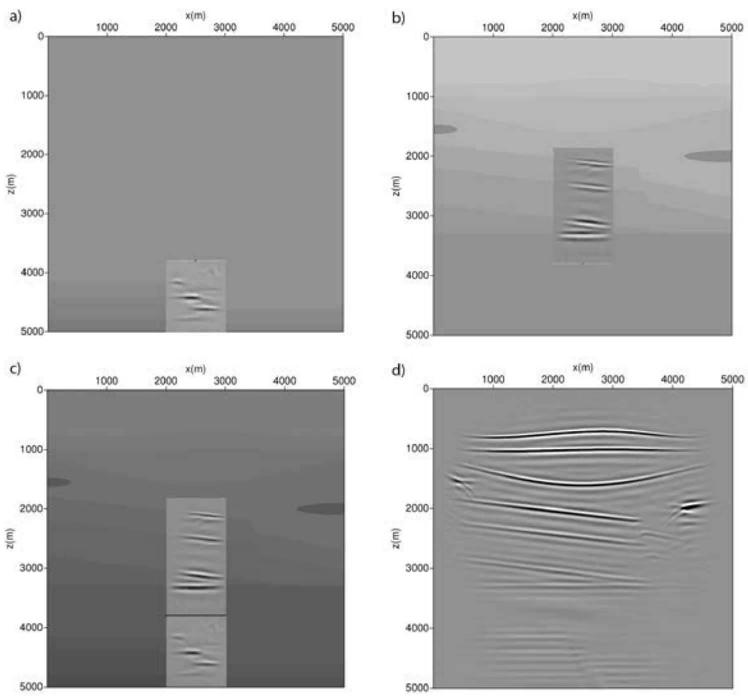

Figure 4: Migration images. a) Migration image of the reflectors below the sources, using the retrieved virtual response by MDD. The background represents the state in which the data is retrieved. b) Migration image of the reflectors aboves above the sources, using the retrieved virtual response by SRI. The background represents the state in which the data is retrieved. c) Combination of both images above and below. The background shows the true velocity model. The polarity of the image above the sources is flipped for consistency with the surface image. d) The migration image using the surface seismic data. The true velocity model is used and a denser source and receiver sampling is used in modelling the data.

REFERENCES

Bakulin, A., and R. Calvert, 2004, 624, *in* Virtual source: new method for imaging and 4D below complex overburden: 2477–2480.

———, 2006, The virtual source method: Theory and case study: Geophysics, **71**, SI139 – SI150.

Berkhout, A. J., 1982, Seismic migration: Imaging of acoustic energy by wave field extrapolation: Elsevier Science Publ. Co., Inc.

Curtis, A., P. Gerstoft, H. Sato, R. Snieder, and K. Wapenaar, 2006, Seismic interferometry - turning noise into signal: The Leading Edge, **25**, 1082 – 1092.

Curtis, A., and D. Halliday, 2010, Source-receiver wave field interferometry: Phys. Rev. E, **81**, no. 4, 046601.

Curtis, A., H. Nicolson, D. Halliday, J. Trampert, and B. Baptie, 2009, Virtual seismometers in the subsurface of the Earth from seismic interferometry: Nature Geoscience, **2**, 700 –704.

Mehta, K., A. Bakulin, J. Sheiman, R. Calvert, and R. Snieder, 2007, Improving the virtual source method by wavefield separation: Geophysics, **72**, V79 – V86.

Poliannikov, O., 2011, Retrieving reflections by source-receiver wavefield interferometry: GEOPHYSICS, **76**, SA1–SA8.

Schuster, G., J. Yu, J. Sheng, and J. Rickett, 2004, Interferometric/daylight seismic imaging: Geophysical Journal International, **157**, 838 – 852.

Snieder, R., K. Wapenaar, and K. Larner, 2006, Spurious multiples in seismic interferometry of primaries: Geophysics, **71**, SI111 – SI124.

Thorbecke, J., and D. Draganov, 2011, Finite-difference modeling experiments for seismic interferometry: GEOPHYSICS, **76**, H1–H18.

Thorbecke, J., K. Wapenaar, and G. Swinnen, 2004, Design of one-way wavefield extrapolation operators, using smooth functions in wlsq optimization: GEOPHYSICS, **69**, 1037–1045.

van der Neut, J., J. Thorbecke, K. Mehta, E. Slob, and K. Wapenaar, 2011, Controlled-source interferometric redatuming by crosscorrelation and multidimensional deconvolution in elastic media: Geophysics, **76**, SA63 – SA76.

Vasconcelos, I., R. Snieder, and B. Hornby, 2008, Imaging internal multiples from subsalt VSP data - Examples of target-oriented interferometry: Geophysics, **73**, S157 – S168.

Wapenaar, K., and J. Fokkema, 2006, Greens function representations for seismic interferometry: Geophysics, **71**, SI33 – SI46.

Wapenaar, K., J. van der Neut, and E. Ruigrok, 2008, Passive seismic interferometry by multidimensional deconvolution: Geophysics, **73**, A51 – A56.

Wapenaar, K., J. van der Neut, E. Ruigrok, D. Draganov, J. Hunziker, E. Slob, J. Thorbecke, and R. Snieder, 2011, Seismic interferometry by crosscorrelation and by multidimensional deconvolution: a systematic comparison: Geophysical Journal International, **185**, 1335 – 1364.